Kinetics of Photoinduced Electron-Transfer Reactions within Sol-Gel Silica Glass Doped with Zinc Cytochrome *c*. Study of Electrostatic Effects in Confined Liquids

Chengyu Shen and Nenad M. Kostić*

Contribution from the Department of Chemistry, Iowa State University, Ames, Iowa 50011

Received June 3, 1996[⊗]

Abstract: Silica hydrogel (glass) was doped with native (iron-containing) cytochrome *c* and with its zinc derivative. Ultraviolet−visible, circular dichroism, and resonance Raman spectra of both proteins and the lifetime of the triplet state of the zinc protein show that encapsulation in the sol-gel glass only slightly perturbs the polypeptide backbone and does not detectably perturb the heme group. Because thermal (ground-state) redox reactions of the encapsulated native cytochrome *c* are very slow, we take advantage of the transparency of the silica to study, by laser flash spectrometry, photoinduced (excited-state) redox reactions of zinc cytochrome *c*, which occur in milliseconds. The triplet state, ^{3}Zncyt, is oxidatively quenched by $[Fe(CN)_6]^{3-}$, dioxygen, and *p*-benzoquinone. These reactions are monophasic in bulk solutions but biphasic in solutions confined in glass. Changes in ionic strength and pH differently affect the kinetics in these two environments. Adsorption of cytochrome *c*, which is positively charged, to the pore walls, which are negatively charged at pH 7.0, affects the kinetics in the doped glass. Exclusion of the $[Fe(CN)_6]^{3-}$ anions from the glass interior also affects the kinetics. Even at equilibrium the anion concentration is lower inside the glass than in the external solution. This exclusion can be lessened or eliminated by raising ionic strength and lowering the pH value. The electroneutral quenchers are not excluded from the glass. Diffusion of all three quenchers is slower in the confined solution than in the bulk solution, as expected. The smaller the molecule, the lesser this hindrance by the glass matrix. In light of these findings, the assumption that porosity of sol-gel glasses ensures uniform penetration of relatively small molecules into the pores must be taken skeptically and tested for each solute (or analyte) of interest, especially for the charged ones. These considerations are important in the design of sensors.

Introduction

Inorganic oxides with chemical compositions of traditional glasses and ceramics can be prepared at room temperature, by polymerization of appropriate precursors.[1−4] This, the sol-gel method, became especially important when it was shown, in the middle 1980s, that the new materials can be doped by various chemicals.[5−13] Since then, many chemical reactions have been effected inside these hydrogels, which we will refer to simply as glasses.[5−11,14−19] The sol-gel method proved compatible with proteins, and several of them, mostly enzymes, have recently been encapsulated in silica glass.[5,14,15,20−32] The method of Avnir and co-workers[24] has been modified by Dunn, Valentine, Zink, and their co-workers,[14,15,20−23] so that noninvassive entrapment of proteins can be achieved relatively easily. Because the pores of hydrogels (partially dried gels) contain water, the protein molecules are solvated and retain their properties.

Sol-gel glasses and composite materials obtained from them have two main properties. Because they are porous, relatively small molecules can move through the pores and reach the relatively large molecules that are trapped inside. Because these glasses are transparent in the UV−visible range, the chemicals and their reactions can be studied by optical spectroscopic

[⊗] Abstract published in *Advance ACS Abstracts,* February 1, 1997.

(1) Brinker, C. J.; Scherer, G. *Sol-gel Science: The Physics and Chemistry of Sol-gel Processing*; Academic Press: San Diego, 1989.
(2) Roy, R. *Science* **1987**, *238*, 1664.
(3) Hench, L. L.; West, J. K. *Chem. Rev.* **1990**, *80*, 33.
(4) Buckley, A. M.; Greenblatt, M. *J. Chem. Educ*. **1994**, *71*, 599.
(5) Avnir, D.; Braun, S.; Lev, O.; Ottolenghi, M. *Chem. Mater*. **1994**, *6*, 1605.
(6) Avnir, D. *Acc. Chem. Res*. **1995**, *28*, 328.
(7) Slama-Schwok, A.; Ottolenghi, M.; Avnir, D. *Nature* **1992**, *355*, 240.
(8) Samuel, J.; Polevaya, Y.; Ottolenghi, M.; Avnir, D. *Chem. Mater*. **1994**, *6*, 1457.
(9) Slama-Schwok, A.; Avnir, D.; Ottolenghi, M. *J. Phys. Chem*. **1989**, *93*, 7544.
(10) Slama-Schwok, A.; Avnir, D.; Ottolenghi, M. *J. Am. Chem. Soc*. **1991**, *113*, 3984.
(11) Levy, D.; Reifeld, R.; Avnir, D. *Chem. Phys. Lett*. **1984**, *109*, 593.
(12) Levy, D.; Avnir, D. *J. Phys. Chem*. **1988**, *92*, 4734.
(13) Tour, J. M.; Cooper; J. P.; Pedalwar, S. L. *Chem. Mater*. **1990**, *2*, 647.
(14) Yamanaka, S. A.; Nishida, F.; Ellerby, L. M.; Nishida, C. R.; Dunn, B.; Valentine, J. S.; Zink, J. I. *Chem. Mater*. **1992**, *4*, 495.
(15) Wu, S.; Ellerby, L. M.; Cohan, J. S.; Dunn, B.; El-Sayed, M. A.; Valentine, J. S.; Zink, J. I. *Chem. Mater*. **1993**, *5*, 115.
(16) Akbarian, F.; Dunn, B.; Zink, J. I. *J. Mater. Chem*. **1993**, *3*, 1041.
(17) Lopez, T.; Moran, M.; Navarrete, J.; Herrera, L.; Gomez, J. *J. Non-Cryst. Solids* **1992**, *147*, 753.
(18) Matsui, K.; Tominaga, M.; Arai, Y.; Satoh, H.; Kyoto, M. *J. Non-Cryst. Solids* **1994**, *169*, 295.
(19) Matsui, K. *Langmuir* **1992**, *8*, 673.
(20) Ellerby, L. M.; Nishida, C. R.; Nishida, F.; Yamanaka, S. A.; Dunn, B.; Valentine, J. S.; Zink, J. I. *Science* **1992**, *255*, 1113.
(21) Dave, B. C.; Soyez, H.; Miller, J. M.; Dunn., B.; Valentine, J. S.; Zink, J. I. *Chem. Mater*. **1995**, *7*, 1431.
(22) Yamanaka, S. A.; Dunn, B.; Valantine, J. S.; Zink, J. I. *J. Am. Chem. Soc*. **1995**, *117*, 9095.
(23) Dave, B. C.; Dunn, B.; Valentine, J. S.; Zink, J. I. *Anal. Chem*. **1994**, *66*, 1120A.
(24) Braun, S.; Rappoport, S.; Avnir, D.; Ottolenghi, M. *Mater. Lett*. **1990**, *10*, 1.
(25) Guo, L.-H.; Mukamel, S.; McLendon, G. *J. Am. Chem. Soc*. **1995**, *117*, 546.
(26) Mabrouk, P. A. *J. Am. Chem. Soc*. **1995**, *117*, 2141.
(27) Glezer, V.; Lev, O. *J. Am. Chem. Soc*. **1993**, *115*, 2533.
(28) Audebert, P.; Demaille, C.; Sanchez, C. *Chem. Mater*. **1993**, *5*, 911.
(29) Zusman, R.; Beckman, D. A.; Zusman, I.; Brent, R. L. *Anal. Biochem*. **1992**, *201*, 103.
(30) Braun, S.; Shtelzer, S.; Rappoport, S.; Avnir, D.; Ottolenghi, M. *J. Non-Cryst. Solids* **1992**, *147*, 739.
(31) Tastu, Y.; Yamashita, K.; Yamagushi, M.; Yamamura, S.; Yamamoto, H.; Yoshikawa, S. *Chem. Lett*. **1992**, *8*, 1615.
(32) Zink, J. I.; Valentine, J. S.; Dunn, B. *New J. Chem*. **1994**, *18*, 1109.

S0002-7863(96)01867-7 CCC: $14.00

methods. A general conclusion from the previous studies is that the trapped compounds retain most of their physical and chemical properties.[6,14,15,20−23]

It is known, however, that liquids confined in porous matrices have special properties.[33,34] In this study we contrast glass interior and bulk solution as media for oxidative quenching of the triplet state of the protein zinc cytochrome *c* by three agents. This work has several features that, to our knowledge, have not been combined before in studies of doped glasses. Transparency has often been used for monitoring, but seldom for initiation, of chemical reactions;[7−10,35−37] we take advantage of transparency and study photoinduced electron transfer from the excited state of a protein to various small molecules.

Sol-gel glasses doped with enzymes and other proteins hold promise as sensors, especially for biomolecules.[20,22,23,27,31,38−41] Quality of these sensors depends on the rate and specificity of protein−analyte interactions, and we report some findings pertinent to this problem. We know of only several quantitative kinetic studies in glasses,[14,15,22,42] all of them recent; much needs to be done in this area. We chose reactions having relatively simple kinetics in aqueous solution and studied kinetics of these reactions inside glass. We found interesting electrostatic effects, which caused unexpected but explainable dependence of rate constants on ionic strength and pH value. These electrostatic effects should be taken into consideration in further research with doped glasses and in their applications as sensors.

Experimental Procedures

Chemicals. Horse-heart cytochrome *c* was obtained from Sigma Chemical Co. Iron(III) ions in the protein were replaced by zinc(II) ions, and the reconstituted protein, designated Zncyt, was purified by a standard procedure, in the dark.[43] The compounds $K_3[Fe(CN)_6]$, tetramethyl orthosilicate (also called tetramethoxysilane), hydroquinone, and *p*-benzoquinone of reagent grade were obtained from Aldrich Chemical Co. The last chemical, which is photolabile, was kept and handled in the dark.[44,45] Ultrapure argon was obtained from Air Products, Inc. Distilled water was demineralized to electrical resistivity greater than 17 MΩ·cm. Sodium phosphate buffer was used throughout; it had pH of 7.0 and concentration of 2.5 mM, unless stated otherwise. Ionic strength (μ) was raised with NaCl and lowered by dilution; it (not the phosphate concentration) is specified.

The Sol-Gel Process. The silica sol was prepared by a published procedure.[15] A 15.76-g sample of tetramethyl orthosilicate and a mixture of 3.38 g of water and 0.22 g of 0.040 M HCl were kept in an ice-cooled ultrasonic bath for 45 min. Clear, homogeneous sol of orthosilicic acid was formed. Upon addition of a 10 mM sodium phosphate buffer at pH 7.0 gelation began. Solutions in the same buffer containing different concentrations of ferricytochrome *c* (the native protein) or of zinc cytochrome *c* (the reconstituted protein) were promptly added to the polymerizing gel. In some experiments the protein was omitted, so that undoped glasses were eventually obtained. The sol, whether doped or undoped, was quickly poured to the height of 10 mm into polystyrene cuvettes (10 × 10 mm) that had all the sides transparent. Rapid polymerization was accompanied by a great increase in viscosity in less than 5 min. Aging and drying continued at 4 °C. During the aging the samples were kept sealed with parafilm, except when methanol was removed, several times a day, by washing with the same sodium phosphate buffer. After 14 days the samples were exposed to air. Drying lasted until 40% by weight of the initially added water evaporated, typically 14−21 days. The hydrogel, which is usually referred to as glass, retained 60% of the water added initially and had 50% of the original volume. The square prismatic slabs (7.5 × 7.5 × 9.0 mm) were stored in a buffer.

Kinetic Experiments. Flash kinetic spectrometry (so-called laser flash photolysis) was done with a standard apparatus.[46] A Phase-R (now Lumenex) laser DL1100 containing a 50 μM solution of rhodamine 590 in methanol delivered 400-ns pulses of polychromatic light with a maximum intensity at 580 nm, perpendicular to the monochromatic probing beam from a tungsten−halogen lamp. The sample was kept under ultrapure argon, in a fluorescence cell (10 × 10 mm). The absorbance−time curves were analyzed with kinetic software from OLIS, Inc. Each signal was an average of eight pulses. Appearance and disappearance of the triplet state of zinc cytochrome *c*, designated ^{3}Zncyt, were monitored at 460 nm, where the transient absorbance reaches the maximum. Appearance and disappearance of the corresponding cation radical, designated $Zncyt^+$, was monitored at 675 nm, where the difference in absorbance between it and the triplet state is greatest. The concentration of zinc cytochrome *c* in the fresh glass (fully hydrated gel) was 10 μM. This concentration in the partially-dried glass, which had shrunk to 50% of its initial volume, was 20 μM. The concentration of ^{3}Zncyt was approximately 1−2 μM and depended on the laser power.

The slabs were soaked for 2−3 days in buffered solutions of a quencher, $K_3[Fe(CN)_6]$ or *p*-benzoquinone. These solutions were changed several times a day, for complete equilibration with the porous glass. The buffer ions, which are relatively small and highly mobile, are assumed to have the same concentration inside the glass and in the external solution. Because the buffer is colorless, movement of its ions between the solution and glass cannot be studied by common experimental methods. Concentrations of the quenchers will be discussed in detail below. Between soakings in different solutions, the slab was thoroughly rinsed by soaking in water.

Each sample for kinetic experiments was thoroughly and noninvasively deaerated in a fluorescence cuvette by gentle flushing with ultrapure argon that had been passed through water in order to avoid evaporation of the solvent and consequent increase in the concentrations of the solutes. When the sample was an aqueous solution, deaeration for ca. 15 min was more than sufficient. When the sample also contained a slab of glass, deaeration lasted 24 h, for complete removal of dioxygen from the pores. Experiments that were done relatively easily with solutions required more effort with glasses. Several days of work, mostly incubation and deaeration of samples, were needed for each point on the linear plots of the observed rate constant versus the quencher concentration, obtained under pseudo-first-order conditions. Three to five of these points defined each linear plot, the slope of which is the second-order rate constant. Finally, these determinations were made at different ionic strengths and pH values. The intricate kinetic experiments with glasses are somewhat less precise than the straightforward experiments with solutions. The estimated errors in the second-order rate constants are ±30% and ±10%, respectively.

Spectroscopic Measurements. Ultraviolet−visible spectra were recorded with an IBM 9430 spectrophotometer. A doped glass in the sample beam was examined against an undoped glass in the reference beam. Each slab was kept in a standard quartz cuvette (10 × 10 mm). The light beams were small enough to pass entirely through the slabs. Circular dichroism spectra at room temperature, measured with a JASCO 710 instrument, gave the ellipticity of protein samples. Ultraviolet−visible spectra of these same samples, measured immediately afterwards, gave the protein concentrations; then molar ellipticity was calculated. Because optical activity decreases with

(33) Xu, S.; Ballard, L.; Kim, Y. J.; Jonas, J. *J. Phys. Chem*. **1995**, *99*, 5787.
(34) Korb, J.-P.; Delville, A.; Xu, S.; Demeulenaere, G.; Costa, P.; Jonas, J. *J. Chem. Phys*. **1994**, *101*, 7074.
(35) Ueda, M.; Kim, H.-B.; Ikeda, T.; Ichimura, K. *Chem. Mater*. **1994**, *6*, 1771.
(36) Ueda, M.; Kim, H.-B.; Ikeda, T.; Ichimura, K. *Chem. Mater*. **1992**, *4*, 1229.
(37) Catellano, F. N.; Heimer, T. A.; Tandhasetti, M. T.; Meyer, G. J. *Chem. Mater*. **1994**, *6*, 1041.
(38) Zusman, R.; Rottman, C.; Ottolenghi, M.; Avnir, D. *J. Non-Cryst. Solids* **1990**, *122*, 107.
(39) Wang, R.; Narang, U.; Bright, F. V. *Anal. Chem*. **1993**, *65*, 2671.
(40) Narang, U.; Prasad, P. N.; Bright, P. N. *Anal. Chem*. **1994**, *66*, 3139.
(41) Dulebohn, J. I.; Haefner, S. C.; Dunbar, K. R. *Chem. Mater*. **1992**, *4*, 506.
(42) Hagen, S. J.; Hofrichter, J.; Eaton, W. A. *Science* **1995**, *269*, 959.
(43) Ye, S.; Shen, C.; Cotton, T. M.; Kostić, N. M. *J. Inorg. Biochem*. and references therein, **1997**, in press.
(44) Ononye, A. I.; Bolten, J. R. *J. Phys. Chem*. **1986**, *90*, 6266.
(45) Ononye, A. I.; Bolten, J. R. *J. Phys. Chem*. **1986**, *90*, 6270.
(46) Zhou, J. S.; Kostić, N. M. *Biochemistry* **1993**, *32*, 4539.

increasing wavelength, progressively higher concentrations were used for the spectra in the following ranges: 200−350, 350−500, and 500−650 nm.

Resonance Raman spectra were measured with a Spex 1807 triple spectrometer equipped with a Princeton Instruments CCD detector, model LN1152, cooled by liquid nitrogen. The excitation source was an Innova 100 Kr^+ laser from Coherent, Inc., emitting at 413.1 nm. The laser power at the samples was less than 5 mW, and radiation was collected in the so-called backscattered configuration, by an *f*/1.2 camera lens. Calibration was done with indene; the resolution was 5 cm^{-1}. The samples were kept in an optical dewar vessel containing liquid nitrogen, and the measurements were made at 77 K.

Porosity of the Glass. Slabs of undoped glass were soaked for several days in solutions containing 100 or 250 μM $K_3[Fe(CN)_6]$ (ϵ_{422} = 1025 M^{-1} cm^{-1}) or 500 μM hydroquinone (ϵ_{297} = 1100 M^{-1} cm^{-1}) in a 600 mM sodium phosphate buffer at pH 7.0. These solutions were changed several times a day. Ultraviolet−visible spectra of the slabs infused with the chromophore were recorded against undoped slabs in the reference beam and then compared with spectra of solutions containing this chromophore in the same buffer. Absorbance ratio for the slab and the solution of the same thickness equals the fraction of the optical path in the glass that passes through the pores, if the pores are filled with the solution. The measurements were repeated with both light beams passing through different parts of the slabs.

Protein Adsorption on Silica. Undoped glass was ground with a pestle in a mortar. To 2.0 mL of a 10 μM solution of ferricytochrome *c* in a 10 mM phosphate buffer at pH 7.0 contained in a spectrophotometric cuvette were added 50 mg of the powdered glass. The suspension was shaken occasionally during 1 day. The UV−vis spectrum of the clear supernatant was compared with the spectrum before addition of the powdered glass. Ionic strength of the supernatant was adjusted to 300 mM with NaCl, and the UV−vis spectra were compared again.

Doped Silica Glass

Formation of Glasses. The sol-gel process remains poorly understood despite many decades of research and application.[1−4,47−52] Different procedures yield gels and glasses of different physical properties. We use a new method, developed by others,[14,15,20] in which acid-catalyzed hydrolysis of $Si(OCH_3)_4$ to $Si(OH)_4$ is promoted by sonication, subsequent condensation polymerization of $Si(OH)_4$ is catalyzed by base, and the gel is never completely dried. The product, sometimes termed hydrogel but usually simply glass, is believed to have properties different from those of xerogels and aerogels.[3,20] In our experiments the rate of gelation increased as temperature and buffer concentration increased. These conditions and also relative volumes of the $Si(OH)_4$ sol and of the sodium phosphate buffer solution at pH 7.0 were adjusted for optimal balance between the probability of cross-linking (i.e., formation of Si−O−Si bonds) and the catalytic efficacy of the phosphate anions. The protein added at the beginning of the gelation had enough time, about 3−5 min, to diffuse uniformly through the viscous solution. Because the polymerization reaction is incomplete, interconnected clusters of silica (SiO_2) are formed, leaving pores in between them. Some of the pores contain molecules of cytochrome *c*, which interrupt polymerization and serve as templates around which this process occurs. Throughout aging and partial drying mechanical strength of the gel increases. As the water evaporates, its fraction decreases and that of the solid increases. The whole gel, and the pores within it, shrink. Consequently, the concentration of the trapped cytochrome *c* doubles, from 10 to 20 μM. Water from the surface pores is lost, and silanol groups at the surface condense. The average pore size in silica xerogel, which is completely dried at high temperature, is ca. 20 Å.[3] The average pores in our glass, which is only partially dried at 4 °C, must be larger than that but smaller than ca. 100 Å because our slabs do not scatter visible light.[20] The partially-dried glass retains enough water to maintain the structure of cytochrome *c*, as will be shown below. Zinc cytochrome *c*, which has very high absorptivity (ϵ_{423} = 2.43 × 10^5 M^{-1} cm^{-1}),[53] was never found in the buffer surrounding the glass, and the absorption spectrum of the protein in the doped glass was essentially the same before and after the incubation. Clearly, the protein does not leak out of the porous glass into the external solution.

Ultraviolet−Visible Spectra and Thermal Oxidoreduction. We confirmed[14,15,20−23] that the undoped glass is optically transparent except for some absorbance around 300 nm; see Supporting Information, Figure 1. Positions and intensities of the hyper, Soret, α, and β bands for both ferricytochrome *c* and zinc cytochrome *c* in the doped glasses remain unchanged throughout the aging and drying process; see Supporting Information, Figures 2 and 3. Uniform color and absorbance of different regions of the doped glass prove homogeneous distribution of the proteins.

When the glasses doped with 20 μM ferricytochrome *c* were immersed first in a 200 μM solution of ascorbic acid and next in a 200 μM solution of $K_3[Fe(CN)_6]$, each of them containing the same sodium phosphate buffer at pH 7.0 as the solvent, complete reduction and then oxidation of the heme iron were clearly evident by the characteristic changes in the UV−vis spectra. This cycle was repeated three times, and each time the spectra of the ferric and ferrous forms of the protein appeared unchanged. We thus confirmed[20] that the encapsulated protein remains capable of reversible redox reactions. Each reaction, however, took 2 days (and each cycle, 4 days) for completion because the redox agents diffused slowly into the porous glass. Much faster reactions are required for further study of doped silica glasses and for their practical applications as sensors. Photoinduced, rather then thermal, redox reactions are promising for both research and application. They are the main subject of this study.

Circular Dichroism Spectra. This spectroscopy has proved very useful in the study of conformation and ligation of heme proteins.[54−57] This and other spectroscopic methods showed that introduction of zinc(II) ions does not appreciably alter the overall structure and conformation of cytochrome *c*.[43,58]

The very strong bands at 209 and 222 nm are due to $\pi-\pi^*$ and $n-\pi^*$ transitions, respectively, in the amide group. These and other features in the so-called intrinsic region, below 300 nm, are the property of the polypeptide backbone and are sensitive indicators of the protein conformation. The strong features in the region 350−500 nm correspond to the Soret absorption band of the heme and are highly sensitive to interactions between this planar chromophore and its chiral environment. The weak circular dichroism in the region 500−

(47) McKiernan, J.; Pouxvier, J.-C.; Dunn, B.; Zink, J. I. *J. Phys. Chem.* **1989**, *93*, 2129.
(48) Pouxvier, J.-C.; Dunn, B.; Zink, J. I. *J. Phys. Chem.* **1989**, *93*, 2134.
(49) Hanna, S. D.; Dunn, B.; Zink, J. I. *J. Non-Cryst. Solids* **1994**, *167*, 239.
(50) Nishida, F.; McKiernan, J. M.; Dunn, B.; Zink, J. I. *J. Am. Ceram. Soc.* **1995**, *78*, 1640.
(51) McKiernan, J. M.; Simoni, E.; Dunn, B.; Zink, J. I. *J. Phys. Chem.* **1994**, *98*, 1006.
(52) Audebert, P.; Griesmar, P.; Hapiot, P.; Sanchez, C. *J. Chem. Mater.* **1992**, *2*, 1293.
(53) Vanderkooi, J. M.; Adar, F.; Erecińska, M. *Eur. J. Biochem.* **1976**, *64*, 381.
(54) Hennessey, J. P.; Johnson, W. C. *Biochemistry* **1981**, *20*, 1085.
(55) Chen, Y.-H.; Yang J. T. *Biochem. Biophys. Res. Commun.* **1971**, *44*, 1285.
(56) Hsu, M.-C.; Woody, R. W. *J. Am. Chem. Soc.* **1971**, *93*, 3515.
(57) Myer, Y. P. *Curr. Top. Bioenerg.* **1985**, *14*, 149.
(58) Anni, H.; Vanderkooi, J. M.; Mayne, L. *Biochemistry* **1995**, *34*, 5744.

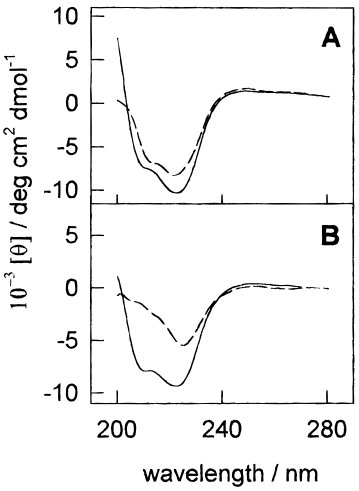

Figure 1. Intrinsic circular dichroism at 25 °C of (A) ferricytochrome *c* and (B) zinc cytochrome *c* in a sodium phosphate buffer at pH 7.0 adjusted with NaCl to ionic strength of 5.0 mM (solid line) and in sol-gel silica glass infused with the same buffer (dashed line). Molar ellipticity is normalized to the mean residue value.

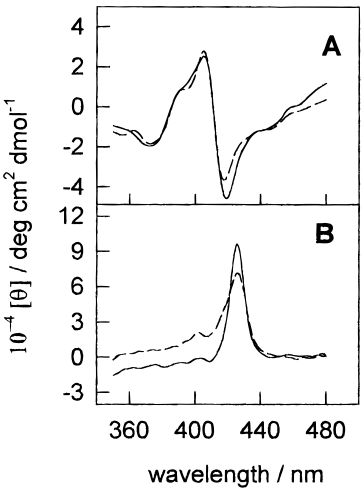

Figure 2. Circular dichroism in the Soret region at 25 °C of (A) ferricytochrome *c* and (B) zinc cytochrome *c* in a sodium phosphate buffer at pH 7.0 adjusted with NaCl to ionic strength of 5.0 mM (solid line) and in sol-gel silica glass infused with the same buffer (dashed line).

650 nm corresponds to the $\pi-\pi^*$ transitions of the heme that are traditionally designated α and β.

As Figure 1 shows, encapsulation of the native and reconstituted cytochrome *c* causes a change in the relative intensity, and a decrease in the absolute intensity, of the intrinsic bands. The approximate extent of α-helicity, estimated with the standard formula,[55,59] is as follows: ferricytochrome *c*, 32 and 28% in solution and glass, respectively; and zinc cytochrome *c*, 30 and 19% in solution and glass, respectively. The spectral changes in zinc cytochrome *c* upon encapsulation are comparable to those caused by electrostatic association of ferricytochrome *c* with highly-charged anions in solution, changes known to be localized and relatively small.[60]

As Figure 2 shows, on encapsulation the Soret spectrum of ferricytochrome *c* changes only slightly, whereas that of zinc cytochrome *c* changes more. The main band in the spectrum of zinc cytochrome *c* broadens, but its position (λ_{max}) does not

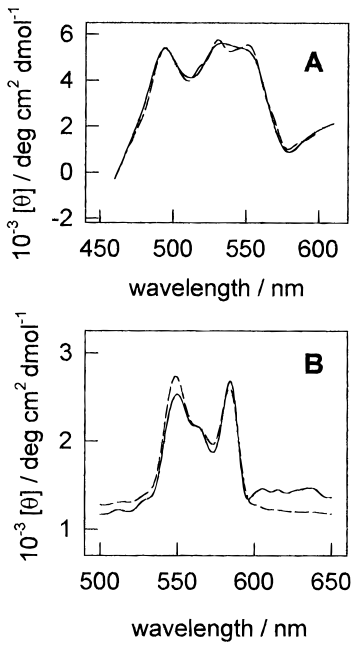

Figure 3. Circular dichroism spectra in the α, β region at 25 °C of (A) ferricytochrome *c* and (B) zinc cytochrome *c* in a sodium phosphate buffer at pH 7.0 adjusted with NaCl to ionic strength of 5.0 mM (solid line) and in sol-gel silica glass infused with the same buffer (dashed line).

change. (Encapsulation causes a similar change in the CD spectrum of bacteriorhodopsin.)[15] Because an edge of the heme group is partially exposed at the surface of cytochrome *c*, even a relatively small conformational change in the crevice containing the heme may affect the CD spectrum.[56,61] If such a conformational change occurs, it must be slight because the spectra in Figure 3 almost overlap.

Resonance Raman Spectra. This spectroscopy has successfully been applied to heme proteins in numerous studies.[62,63] Laser excitation at wavelengths within electronic absorption bands of the heme can cause great enhancement of the vibrational modes of the heme. In a recent study our collaborators and we applied this method for the first time to zinc cytochrome *c* and showed that the size of the porphyrin "core" is inconsistent with six-coordination and is consistent with five-coordination. Unlike the iron(II) and iron(III) ions, which have both His 18 and Met 80 as axial ligands, the zinc(II) ion in cytochrome *c* seems to have only one axial ligand, probably His 18.[43] This difference in coordination number between the native and reconstituted proteins is retained in the glass.

This study concerns the effects of encapsulation. As Table 1 shows, all the vibrational bands have identical wavenumbers, within the error bounds of the experiment, in solution and in glass. Even the relative intensities of most of the bands remain unchanged. There are some exceptions to this generalization. The relative intensities of pairs of bands of zinc cytochrome *c* are as follows: in solution, 3:4 for the bands at 756 and 728 cm^{-1} and 2:1 for the bands at 698 and 682 cm^{-1}; in the glass, 1:1 for the bands at 755 and 726 cm^{-1} and 1:1 for the bands at 697 and 680 cm^{-1}. These minor changes in the relative intensities notwithstanding, the glass matrix does not appreciably alter the spin state, oxidation state, and geometry of the heme site.

(59) Benson, D. R.; Bradley, R. H.; Doughty, M. B. *J. Am. Chem. Soc.* **1995**, *117*, 8502.
(60) Chottard, G.; Michelon, M.; Herve, M.; Herve, G. *Biochem. Biophys. Acta* **1987**, *916*, 402.
(61) Mizutini, T.; Tadashi, E.; Ogoshi, H. *Inorg. Chem.* **1994,** *33*, 3558.
(62) Hildebrandt, P. In *Cytochrome c: a Multidisciplinary Approach*; Scott, R. A., Mauk, A. G., Eds.; University Science Books: Sausalito, CA, 1996; Chapter 6.
(63) Hu, S.; Morris, I. K.; Singh, J. P.; Smith, K. M.; Spiro, T. G. *J. Am. Chem. Soc.* **1993**, *115*, 12446 and references therein.

Table 1. Resonance Raman Bands of Ferricytochrome *c* and of Zinc Cytochrome *c* in Solution and in Partially-Dried Silica Gel

	wavenumber/cm^{-1}			
	cyt(III)		Zncyt	
assignment[a]	solution	glass	solution	glass
υ_{10}	1641	1642	1614	1613
υ_2			1591	1591
υ_{19}	1589	1591		
υ_3	1507	1508	1481	1481
υ_4	1375	1376	1369	1369
υ_{30}	1177	1176	1176	1176
υ_{43}			1141	1142
υ_{14}	1129	1128		
$\delta(C_bH_3)_{2,4}$			1052	1052
$\upsilon(C_cC_d)_{6,7}$	971	971	969	971
υ_6			799	797
υ_{15}	748	748	756	755
γ_5	731	731	728	726
υ_7	701	701	698	697
$\upsilon(C_aS)$			682	680
γ_{21}	569	568	577	576
γ_{12}	522	522	520, 510	511
υ_{33}	481	480		
γ_{22}	445	447	451	448
$\delta(C_\beta C_aC_b)_{2,4}$	415	415	421, 411	411
$\delta(C_\beta C_aS)$	400	399		
$\delta(C_\beta C_cC_d)_{6,7}$	379	381	384, 375	385, 374
υ_8	351	350	342	342
υ_{51}	307	307		
υ_9	270	270		

[a] Reference 63.

Lifetime of the Triplet State. The rate constant for natural decay of ^{3}Zncyt in aqueous solution is 100 ± 10 s^{-1} throughout the intervals $5.0 \leq$ pH ≤ 9.0 and 2.5 mM $\leq \mu \leq 3.00$ M.[64] The rate constant for the encapsulated zinc cytochrome *c* at pH 7.0 is 70 ± 10 s^{-1}. This slight decrease, corresponding to a slight increase in the lifetime of the triplet state (Supporting Information, Figure 4), indicates a small stabilization of the protein in the glass. The decrease in the rate constant is probably caused by immobilization, which lessens the probability of collisions involved in quenching the excited state.

Quenching of ^{3}Zncyt by the $[Fe(CN)_6]^{3-}$ Anion

The Reaction. Because zinc(II) is a redox-inactive ion, zinc cytochrome *c* in its ground electronic state cannot react with the $[Fe(CN)_6]^{3-}$ ion. In other words, thermal electron-transfer reaction is not possible. Because, however, the triplet state of the porphyrin ring is a strong reducing agent, the reaction in eq 1 is readily induced by a laser pulse.[65] Because the cation radical of the porphyrin in Zncyt$^+$ is a strong oxidizing agent, reverse electron transfer regenerates zinc cytochrome *c* (in the ground state) and $[Fe(CN)_6]^{3-}$. The next laser pulse triggers another sequence of two electron transfers in opposite directions, and so on.

$$^3\text{Zncyt} + [Fe(CN)_6]^{3-} \xrightarrow{k} \text{Zncyt}^+ + [Fe(CN)_6]^{4-} \quad (1)$$

The net charges of the two reactants in eq 1 are 6+ and 3− at pH 7.0. (Electrostatic repulsion between the cytochrome *c* molecules and redox-inactivity of the zinc(II) ion preclude "self-quenching" by electron transfer.) Effects of ionic strength on the second-order rate constant *k* give information about electrostatic interactions of these two molecules with each other and with their environment. We are particularly interested in the properties of the glass interior, that is, in the possible difference between the hydrated pores and the bulk solution.

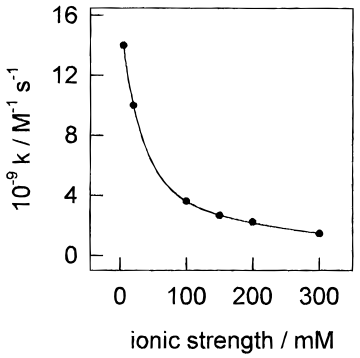

Figure 4. Dependence on ionic strength of the second-order rate constant for the reaction in eq 1 in a sodium phosphate buffer at pH 7.0 containing variable concentration of NaCl, at 25 °C.

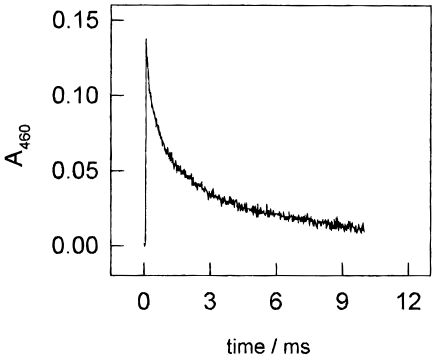

Figure 5. Decay of the triplet state ^{3}Zncyt in sol-gel glass, in the presence of 100 μM $[Fe(CN)_6]^{3-}$ complex as the quencher. The solvent is a sodium phosphate buffer at pH 7.0 adjusted with NaCl to ionic strength of 20 mM.

The Reaction in Solution. As Figure 4 shows, the rate constant *k* increases from 1.0×10^9 to 1.4×10^{10} M^{-1} s^{-1} as the ionic strength of the buffered solution decreases from 300 to 5.0 mM owing to the attraction between the reactants. Electrostatic interactions between redox metalloproteins and transition-metal complexes have been much studied in the past and are largely understood.[66,67] Without revisiting solved problems, we point out that the disappearance of ^{3}Zncyt in bulk solution is a monoexponential process characterized by monotonic dependence of the rate constant on ionic strength. The only important interaction in solution seems to be the attraction between the reactants in eq 1.

The Reaction in Glass. A slab of glass uniformly doped with 20 μM zinc cytochrome *c* was thoroughly equilibrated with $K_3[Fe(CN)_6]$. The triplet state, ^{3}Zncyt, is created in situ by a laser flash. Because its quenching is controlled by local diffusion within the pores, not by transfer of the $[Fe(CN)_6]^{3-}$ ions from the bulk solution to the glass interior, the reaction in eq 1 is fast. It was followed by monitoring both the disappearance of the triplet state (see Figure 5) and the appearance of the cation radical (see Supporting Information, Figure 5). Because the sol-gel glass is not perfectly transparent (see Supporting Information, Figure 1), some excitation photons are scattered and the latter trace is noisy. Because a fraction of ^{3}Zncyt in the pores may be inaccessible to the quencher, the

(64) Zhou, J. S.; Kostić, N. M. *J. Am. Chem. Soc.* **1993**, *115*, 10796.
(65) Shen, C.; Kostić, N. M. *Inorg. Chem.* **1996**, *35*, 2780.
(66) Wherland, S.; Gray, H. B. In *Biological Aspects of Inorganic Chemistry*; Dolphin, D., Ed.; Wiley: New York, 1977; p 298.
(67) Moore, G. R.; Eley, C. G. S.; Williams, G. *Adv. Inorg. Bioinorg. Mech.* **1984**, *3*, 1.

signal of $Zncyt^+$ is diminished. Nevertheless, detection of the cation radical indicates that the triplet state is quenched by the electron-transfer reaction, according to eq 1.

The trace in Figure 5 cannot be fitted with one or two exponentials but can be fitted well with three exponentials of approximately equal amplitudes. (This seems to be an important property of chromophores encapsulated in sol-gel glasses. Luminescence of both an organic compound[8] and a metal complex[9] is highly nonexponential.) Excellent fitting can, of course, be obtained also with more than three exponentials. The slowest process, having the rate constant of 100−200 s^{-1} in different experiments, is the natural decay of ^{3}Zncyt, probably in somewhat different environments. The observed rate constants of the other two exponential components changed with varying concentration of the quencher, as expected, but that of the faster component remained approximately eight times greater than that of the slower. Both of these components correspond to the quenching according to eq 1. The contrast between the monophasic quenching in solution and multiphasic quenching in silica glass highlights the difference between the homogeneous free solution and the microheterogeneous environment in the pores.

Kinetic Effects of Ionic Strength in Glass. Two typical pseudo-first-order kinetic plots (in each case, for the faster of the two exponential components) are shown in the Supporting Information, Figure 6. The rate constant decreased from 6.3 × 10^7 to 2.5 × 10^7 M^{-1} s^{-1} as the ionic strength decreased from 60 to 20 mM. (The slower component showed a similar decrease.) These findings, and others of their kind that are not shown in figures, define a trend opposite to that found in solution (Figure 4). Although the quenching reaction inside the glass is relatively fast, it is much slower than the reaction in solution. The respective rate constants at the ionic strength of 20 mM are 2.5 × 10^7 (for the faster component) and 1.1 × 10^{10} M^{-1} s^{-1}. The causes of this ca. 400-fold decrease will be discussed later. First, we discuss the surprising effect of ionic strength.

Each quartet of data points in Figure 6 is the result of approximately 1 week's work. The second-order rate constants were obtained reproducibly with the same slab of doped glass, so that the concentration of encapsulated zinc cytochrome *c* was kept constant. Clearly, all the dialysis experiments were reversible, and the reaction in eq 1 did not cause any permanent change in the glass. Some of the points were also reproduced with another slab of doped glass. As Figures 6A and 6B show, the rate constants for the two components depend identically on ionic strength (assumed to be the same inside the glass and in external solution): no change or a slight increase from 600 to 100 mM and a steep decrease down to 10 mM. The rate constants of the two components remain in the approximate ratio of 8:1, and their amplitudes remain approximately equal, at all ionic strengths. In the following discussion we will offer an explanation for the intriguing contrast between the effects of ionic strength in solution and in the pores of the silica glass.

Adsorption of Cytochrome *c* on the Silica Surface. Silica surface and therefore the pore walls contain functional groups of several kinds: siloxane (Si−O−Si), silaketone (Si═O), silanol (Si−OH), and siloxide (Si−O^-).[68] Because these groups exist in variable proportions and individually or in clusters of various sizes, the pK_a values of silica gel span the interval 3 < pH < 9.[69,70] Silica gel and the sol-gel glass bear a net negative charge at pH 7.0. Ferricytochrome *c* and zinc cytochrome *c* have net charges of 7+ and 6+, respectively, at pH 7.0.[67] Very

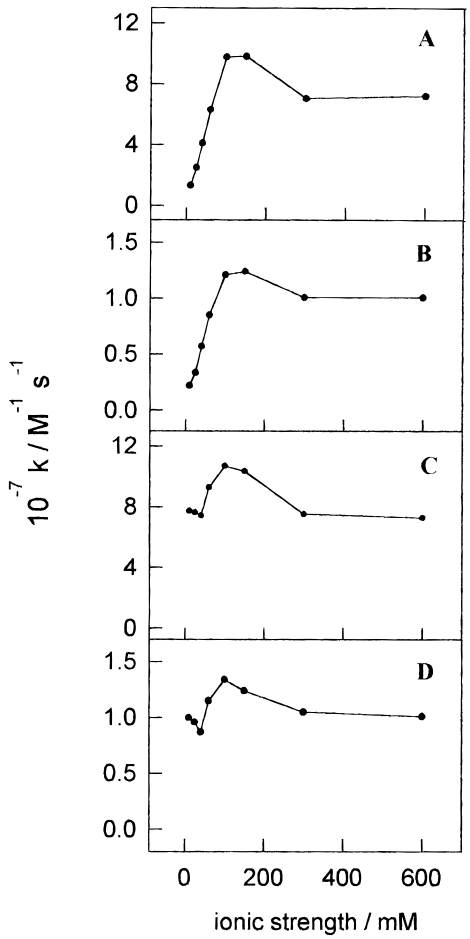

Figure 6. Dependence on ionic strength of the second-order rate constant for the faster (A, C) and slower (B, D) components of the reaction in eq 1 inside sol-gel silica glass infused with a sodium phosphate buffer at pH 7.0 containing variable concentration of NaCl: (A and B) assuming that the $[Fe(CN)_6]^{3-}$ concentration inside the glass equals that in the external solution of $K_3[Fe(CN)_6]$; (C and D) recognizing the partial exclusion of the $[Fe(CN)_6]^{3-}$ ions from the glass interior at ionic strength lower than 600 mM and correcting their concentration inside the glass according to eq 2.

recent measurements of dipolar relaxation of ferricytochrome *c* in silica glass at pH 4.25 and ionic strength of 100 mM showed that encapsulation slightly restricts the movement of the protein molecules. Since the activation energy for this relaxation is only 1.1 kcal/mol greater inside the glass than in solution, rotation of the protein molecules inside the glass at pH 4.25 and ionic strength of 100 mM is almost as free as that in solution.[21]

In our experiments, at pH 7.0 and ionic strength of 10 mM, UV−vis absorption of ferricytochrome *c* solution disappeared upon incubation with powdered undoped glass, which became reddish. Evidently, the protein was completely removed from solution and adsorbed on the glass.[71,72] Raising the ionic strength restored only a part of the original UV−vis absorbance. These qualitative experiments show that adsorption at pH 7.0 is relatively strong and only partially reversible.

Selected rate constants shown in Figures 6A and 6B were reproduced with the same slab of doped glass when the ionic strength was raised and then lowered. The apparent small increase in the rate constant *k* as the ionic strength decreases

(68) Ramsden, J. T. *Chem. Soc. Rev.* **1995**, 74.
(69) Hair, M. L.; Hertl, W. *J. Phys. Chem.* **1970**, *74*, 91.
(70) Schrindler, P.; Dick, R.; Wolf, P. *J. Colloid Interface Sci.* **1976**, *55*, 469.
(71) Duinhoven, S.; Poort, R.; Van Der Voet, G.; Agterof, W. G. M.; Norde, W.; Lyklema, J. *J. Colloid Interface Sci.* **1995**, *170*, 340.
(72) Duinhoven, S.; Poort, R.; Van Der Voet, G.; Agterof, W. G. M.; Norde, W.; Lyklema, J. *J. Colloid Interface Sci.* **1995**, *170*, 351.

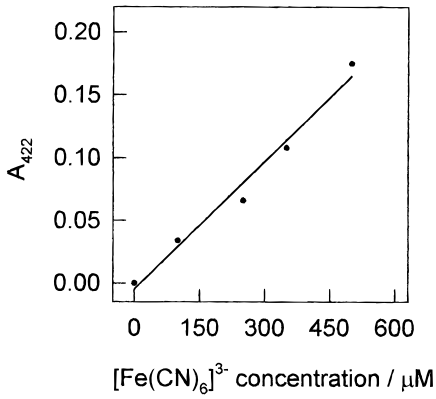

Figure 7. Uptake of the $[Fe(CN)_6]^{3-}$ complex by a slab of undoped sol-gel glass immersed in solutions containing different concentrations of the complex. The solvent is a sodium phosphate buffer at pH 7.0 adjusted with NaCl to ionic strength of 20 mM.

from 600 to 100 mM is qualitatively consistent with the behavior expected of oppositely-charged reactants in eq 1 that are mobile inside the glass pores. The steep decrease of the rate constant upon further lowering of ionic strength is consistent with the hypothesis of adsorption of zinc cytochrome *c* on the pore walls. The exposed heme edge, through which an electron is given to the $[Fe(CN)_6]^{3-}$ ion, is surrounded by a ring of positively-charged amino-acid side chains.[67] If this basic patch adhered to the negatively-charged surface of the pore, the heme edge would become less accessible to the quencher; this attraction is expected to be favored at low ionic strengths. The two components of the reaction cannot be due to the adsorbed and unadsorbed protein because the relative amplitudes of these components are independent of ionic strength.

Exclusion of $[Fe(CN)_6]^{3-}$ Ions from the Glass. Partial adsorption of zinc cytochrome *c* on the pore walls is not the only possible cause of the unexpected dependence in Figures 6A and 6B. The second-order rate constant depends also on the concentration of the $[Fe(CN)_6]^{3-}$ ion. Because this octahedral anion is much smaller than 20 Å, the estimated lower limit of the pore size, it is reasonable to assume that uniform diffusion of this quencher into the glass is not obstructed by steric factors. Considering relative sizes, prolonged immersion of a slab of glass in fresh batches of the same $K_3[Fe(CN)_6]$ solution is expected to yield equal concentrations of the $[Fe(CN)_6]^{3-}$ ions in the pores ("inside") and in the solution ("outside"). Size, however, is not the only relevant factor.

The kinetic experiments in this section were done with two different slabs of undoped glass. The results were consistent, and only one set is shown in Figure 7. Each slab was dialyzed against solutions containing various (constant) concentrations of $K_3[Fe(CN)_6]$ in sodium phosphate buffers at pH 7.0 having various (constant) ionic strengths. Soaking was ended when the UV−vis spectrum of the glass ceased changing, i.e., when equilibrium was reached. Between dialyses against different solutions, the slab was thoroughly rinsed by soaking in water. For the same concentration of the $[Fe(CN)_6]^{3-}$ ions in solution, the greater the ionic strength, the greater the absorbance of these ions inside the glass. Since the absorptivity ($\epsilon_{422} = 1025\ M^{-1}\ cm^{-1}$) of $[Fe(CN)_6]^{3-}$ is independent of ionic strength in the range used in these experiments, it is reasonable to assume that the absorptivity in bulk solution applies also to the confined solution. Evidently, uptake of $[Fe(CN)_6]^{3-}$ by the glass increases as ionic strength increases. At a constant ionic strength (to which $K_3[Fe(CN)_6]$ contributed much less than NaCl) absorbance at 422 nm of the glass was directly proportional to the concentration of $[Fe(CN)_6]^{3-}$ ions in the external solution; see Figure 7. The slope of this plot of absorbance "inside" vs concentration "outside" was, however, only about one-third the absorptivity of the $[Fe(CN)_6]^{3-}$ ions. This was additional evidence for partial exclusion of the anion from the glass interior.

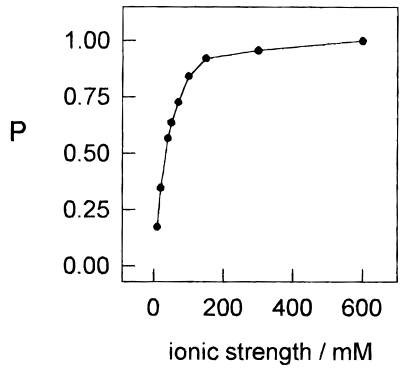

Figure 8. Dependence on ionic strength of the partitioning coefficient, *P*, for $[Fe(CN)_6]^{3-}$ ions between the interior of the sol-gel glass and the external solution. For definition, see eq 2. The solvent was a sodium phosphate buffer at pH 7.0 containing variable concentration of NaCl.

Porosity of the Glass. At the ionic strength of 600 mM electrostatic interactions are negligible. Repulsion between the silica surface and the $[Fe(CN)_6]^{3-}$ anions, and therefore also exclusion, is presumed absent. Nevertheless, absorbance of these anions in undoped glass never equaled that of a surrounding solution having the same thickness (optical path length). Experiments with four different undoped slabs, prepared by the same procedure at different times, gave relative absorbances at 422 nm (in comparison with solutions in which they were incubated for 3 days) of 0.822, 0.843, 0.870, and 0.898. These values were independent of the $K_3[Fe(CN)_6]$ concentration in the surrounding solution. Absorbances remained unchanged when different parts of each slab were probed by the light beam. Evidently, all the slabs were optically isotropic and uniformly infused with $[Fe(CN)_6]^{3-}$ ions, but they differed in porosity. The solution can enter only into the pores of the glass; silica itself is transparent but impenetrable. Cubes of the aforementioned path length factors (relative absorbances) yielded the following respective estimates of the pore volume as the percentage of the slab volume: 56, 60, 66, and 72%. Small variation in the path length factor corresponds to a larger variation in the estimated volume of the pores, but the results are qualitatively consistent.

Similar experiments, lasting 4 days, were done also with hydroquinone, an electroneutral species. Two different undoped slabs gave path length factors (relative absorbances) at 315 nm of 0.90 and 0.94, corresponding to the estimated pore volumes of 72 and 83%, respectively. The smaller molecules seem to penetrate the pores more fully, as might be expected.

Partitioning Coefficient. Given the path length factor, concentration C_{in} of a solute in the glass can be determined from its UV−visible spectrum. The concentration C_{out} in the external solution is known. Partitioning coefficient is defined simply in eq 2. This coefficient for $[Fe(CN)_6]^{3-}$ ions is plotted in Figure 8. Consistent plots were obtained with two different slabs of glass; one of these is shown.

$$P = C_{in}/C_{out} \tag{2}$$

Corrected Effects of Ionic Strength in Glass. The second-order rate constants *k* in Figures 6A and 6B for the electron-transfer reaction in glass were calculated with $[Fe(CN)_6]^{3-}$ concentrations in external solution, C_{out}. The unexpectedly low rate constants at low ionic strength may be due to partial

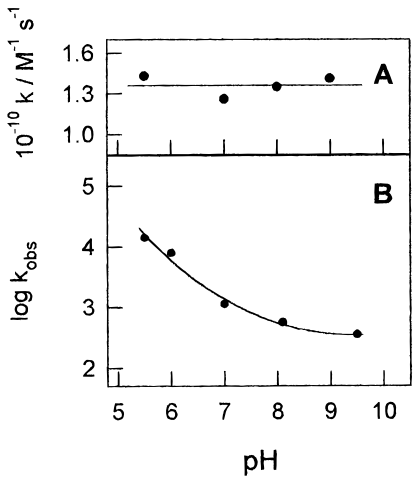

Figure 9. Kinetics of the reaction in eq 1 at various pH values of the bulk solution, at ionic strength of 7.5 mM. (A) Independence of the second-order rate constant for the reaction in bulk solution. (B) Dependence of the pseudo-first-order rate constant for the reaction in sol-gel silica glass.

exclusion of the $[Fe(CN)_6]^{3-}$ ion from the glass interior. When the rate constants were recalculated with corrected concentrations of the quencher, C_{in}, Figures 6C and 6D were obtained. The surprising feature at low ionic strength disappeared, but Figures 6C and 6D still differ greatly from Figure 4 in that the rate constant in the glass does not significantly increase as ionic strength decreases. The remaining small hump in Figures 6C and 6D lies within the error bounds of the kinetic experiments with glasses; the rate constant can be considered virtually independent of ionic strength.

This independence may perhaps be attributed, at least in part, to adsorption of the protein to the pore walls at low ionic strength. Because the charge of the protein is neutralized by the charge of the surface, electrostatic interactions between the reactants are absent. When the protein is desorbed from the pore walls, its electrostatic interactions with $[Fe(CN)_6]^{3-}$ ions are still weak or absent because of the high ionic strength required for desorption. Glass interior is intrinsically different from bulk solution as a medium for the reaction in eq 1 and possibly for other reactions.

Kinetic Effects of pH in Glass. Because the experiments discussed above were done mostly at medium and high ionic strengths, the reactions were relatively fast. The following experiments were done at a low ionic strength of 7.5 mM, so that exclusion effects are pronounced. As Figure 9A shows, the reaction in bulk solution does not depend on the pH value. Indeed, conformation of cytochrome *c* remains the same, and its net charge varies only slightly, in the interval $5.5 \leq$ pH ≤ 9.0. The reaction in glass, however, appears to be assisted by a decrease of pH; see Figure 9B. The partitioning coefficient (eq 2) for $[Fe(CN)_6]^{3-}$ ions at the ionic strength of 7.5 mM and at $7.0 \leq$ pH ≤ 9.5 is very low. Consequently, the quenching reactions at the ionic strength of 7.5 mM are slow. The partitioning coefficient is larger in weakly acidic solutions: 0.35 and 0.38 at pH values of 6.0 and 5.5, respectively. Evidently, the exclusion discussed above can be lessened even at low ionic strength by (partial) protonation of the negatively-charged siloxide groups on the silica surface. The difference between Figures 9A and 9B reflects an intrinsic difference between solution and sol-gel glass as reaction media.

Quenching of ^{3}Zncyt by Electroneutral Molecules

We showed above that cytochrome *c* can adsorb on the silica surface but explained the surprisingly low rate constants at low ionic strength (Figures 6A and 6B) in terms of other factors. To verify this explanation, we studied reactions with the electroneutral quenchers dioxygen (eq 3) and *p*-benzoquinone (eq 4). As before, the reverse electron-transfer reactions, which are not shown, regenerated the reactants and allowed repeated flashing of the same slab. As before, the slowest of the three exponential components was the natural decay of the triplet state. As before, the other two exponentials corresponded to the quenching reaction, and the faster component had the rate constant approximately seven times that of the slower.

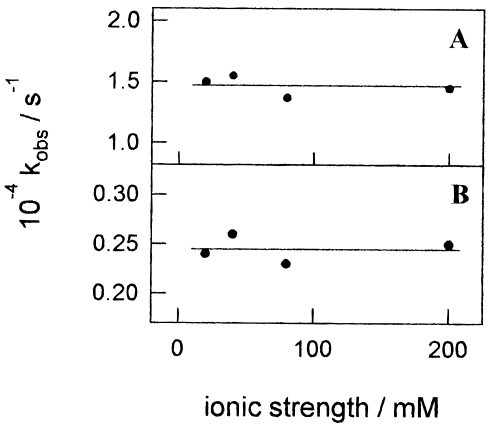

Figure 10. Independence of ionic strength of the pseudo-first-order rate constant for the reaction in eq 3 in sol-gel silica glass: (A) the faster component; (B) the slower component.

$$^3\text{Zncyt} + O_2 \xrightarrow{k_{obs}} \text{Zncyt}^+ + O_2^- \quad (3)$$

$$^3\text{Zncyt} + \text{O=C}_6\text{H}_4\text{=O} \xrightarrow{k} \text{Zncyt}^+ + {}^\bullet\text{O-C}_6\text{H}_4\text{-O}^- \quad (4)$$

Reaction with Dioxygen. Because concentration of dioxygen in water is fixed by the solubility of air, the quantities plotted in Figure 10 are the observed, not the second-order, rate constants for both components of the reaction in eq 3. Their independence of ionic strength was an interesting, albeit preliminary, evidence concerning the interactions in the confined solution.

Reaction with *p*-Benzoquinone. Diffusion of this compound into glass was studied as described above for $K_3[Fe(CN)_6]$. Ultraviolet absorbance ($\epsilon_{305} = 225$ M^{-1} cm^{-1}) inside the glass is directly proportional to concentration of *p*-benzoquinone in external solutions; see Supporting Information, Figure 7. There is no exclusion. The partitioning coefficient (eq 2) is equal to one, within the margins of experimental error, in the entire range 20 mM $\leq \mu \leq$ 300 mM; see Supporting Information, Figure 8. The second-order rate constants for the faster and the slower components of the reaction in eq 4 are 1.4×10^8 and 2.0×10^7 M^{-1} s^{-1} in the entire interval 20 mM $\leq \mu \leq$ 300 mM; see Figure 11.

The results in Figures 10 and 11 show that availability of zinc cytochrome *c* molecules for the reaction inside glass pores is not significantly affected by adsorption to the pore walls. If this is true also for the reaction in eq 1, then the small humps in Figures 6C and 6D, which lie within the error margins of the kinetic experiments with glass, are insignificant. Our conclusion above is now confirmed. The interesting effects of low ionic strength on the reaction in eq 1 within glass are due to partial exclusion of the anionic quencher from the glass interior.

Hindrance of Diffusion in Glasses

Even the solutes that are small enough to penetrate the glass uniformly may be somewhat retarded by this matrix in chemical

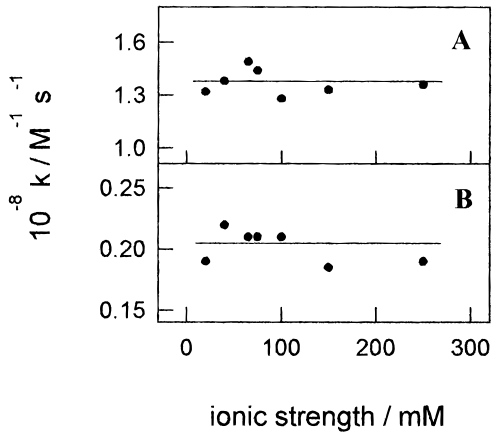

Figure 11. Independence of ionic strength of the second-order rate constant for the reaction in eq 4 in sol-gel silica glass: (A) the faster component; (B) the slower component.

reactions. We compared the rate constants for the reactions in eqs 1, 4, and 3 in bulk solution and in solution confined within glass. In each case the latter reaction was slower than the former. The ratio of the rate constant in solution and the rate constant of the faster component in glass (the hindrance factor of the glass) decreased as the quencher for ^{3}Zncyt became smaller and more mobile. At the ionic strength of 20 mM these factors for $[Fe(CN)_6]^{3-}$, *p*-benzoquinone, and O_2 are 400, 5, and 1.1, respectively. At the ionic strength of 300 mM, at which electrostatic effects are minimized, the hindrance factors are 20, 5, and 1.1, respectively. Although $[Fe(CN)_6]^{3-}$ and *p*-benzoquinone are relatively small molecules, their movement is retarded by the glass environment. Again, solutes behave differently in bulk solution and in solution confined inside the pores.

A recent study of diffusion of liquids in sol-gel silica, by methods quite different from out kinetic measurements, yielded hindrance factors in the range 4−8 for small, neutral molecules.[73] Our value of 5 for *p*-benzoquinone nicely falls in this interval. These other methods have yet to be applied to ions.

Because the pores in a sol-gel glass are not straight, species diffusing in confined liquids cover a longer distance than they would in homogeneous liquids. The pore connectivity and the effective path length are discussed in terms of the tortuosity factor.[74] Our findings are consistent with these new concepts.

Conclusions

This study confirms the utility of the new sol-gel method for doping silica glass with proteins. Because the glasses are optically transparent, they are well suited to the study of photoinduced chemical reactions. Kinetic investigation of these fast reactions revealed some interesting and important properties of sol-gel silica, which should be taken into account when it is used as a matrix for sensors.

Because the silica surface may be charged, diffusion of ions between the glass and surrounding solution may result in different ion concentrations in these two domains even when the system has reached equilibrium. The concentrations at equilibrium may depend on pH and ionic strength, factors that determine the surface charge. Quantitative theoretical study of these effects has only begun.[75−77] Because of them, the common assumption that porosity of sol-gel glasses ensures uniform penetration of relatively small species into the pores must be taken skeptically and tested for each solute of interest, preferably at different concentrations of this solute and under different conditions of ionic strength, pH, and other relevant factors. Microscopic heterogeneity of the glass interior and multiphasic kinetics of reactions occurring there are recognized[8,9,73,74] as important factors. This study contributes to the understanding of these phenomena.

Acknowledgment. This work was supported by the NSF, through Grant No. MCB-9222741. Chengyu Shen thanks Mrs. Neoma Wall for a graduate fellowship. We thank Dr. George Chumanov and Shuyu Ye, who recorded the resonance Raman spectra.

Supporting Information Available: Ten figures, showing the absorption spectrum of undoped glass, evolution of the absorption spectrum of glasses doped with ferricytochrome *c* and with zinc cytochrome *c* during gelation and drying, natural decay of ^{3}Zncyt in solution and in glass, kinetic profile of the cation $Zncyt^+$ formed upon quenching of ^{3}Zncyt by $[Fe(CN)_6]^{3-}$ ions in the glass, dependence on ionic strength of the rate constant for the fastest component of quenching of ^{3}Zncyt by $[Fe(CN)_6]^{3-}$ ions in glass, independence of ionic strength of the rate constant for quenching of ^{3}Zncyt by O_2 in solution, uptake of *p*-benzoquinone by undoped glass, lack of partitioning of *p*-benzoquinone between the glass and solution at different ionic strengths, and independence of ionic strength of the rate constant for quenching of ^{3}Zncyt by *p*-benzoquinone in solution (7 pages). See any current masthead page for ordering and Internet access instructions.

JA961867T

(73) Koone, N.; Shao, Y.; Zerda, T. W. *J. Phys. Chem.* **1995**, *99*, 16976.
(74) Sieminska, L.; Zerda, T. W. *J. Phys. Chem.* **1996**, *100*, 4591.
(75) Dubois, M.; Zemb, J.; Belloni, L.; Setton, R. *J. Chem. Phys.* **1992**, *96*, 2287.
(76) Vlachy, V. I.; Haymet, A. D. *Aust. J. Chem.* **1990**, *43*, 1961.
(77) Jamnik, B.; Vlachy, V. *J. Am. Chem. Soc.* **1995**, *117*, 8010.